

Perspectives on various-temperature stability of p-i-n perovskite solar cells

Cite as: Appl. Phys. Lett. **126**, 010502 (2025); doi: 10.1063/5.0245576

Submitted: 28 October 2024 · Accepted: 13 December 2024 ·

Published Online: 2 January 2025



Ying Tang,^{1,2} Yufang Liu,^{1,3,a)} and Meng Li^{2,a)}

AFFILIATIONS

¹School of Physics, Henan Normal University, Xinxiang 453007, People's Republic of China

²Key Lab for Special Functional Materials of Ministry of Education, National & Local Joint Engineering Research Center for High-efficiency Display and Lighting Technology, School of Nanoscience and Materials Engineering, and Collaborative Innovation Center of Nano Functional Materials and Applications, Henan University, Kaifeng 475004, People's Republic of China

³Institute of Physics, Henan Academy of Sciences, Zhengzhou 450046, People's Republic of China

^{a)}Authors to whom correspondence should be addressed: yf-liu@htu.edu.cn and mengli@henu.edu.cn

ABSTRACT

Despite the significant breakthroughs in photoelectric conversion efficiency achieved by perovskite solar cells, their temperature stability remains a significant bottleneck to commercialization. Temperature fluctuations typically lead to structural changes and phase transformations in perovskites. Additionally, thermal stress can facilitate ion migration within the perovskite material, resulting in interface charge accumulation and electrode corrosion, which ultimately undermines the performance of perovskite devices. This brief perspective systematically discusses the mechanisms behind device performance degradation under temperature cycling conditions and presents potential improvement strategies to address these issues. Finally, we elaborate on the future challenges that must be overcome for the successful commercialization of these devices.

Published under an exclusive license by AIP Publishing. <https://doi.org/10.1063/5.0245576>

I. INTRODUCTION

Perovskite solar cells (PSCs) are currently at the forefront of next-generation photovoltaic technology due to their remarkable photoelectric performance, low cost, and facile processability.^{1,2} At present, the state-of-art PSCs have reached a power conversion efficiency (PCE) of 26.7%³ which is now competitive with that of silicon photovoltaic cells.⁴ Despite the tremendous achievements that have been made in PSCs, long-term operational stability is still the main obstacle to the commercialization of PSCs.⁵ As we all know, perovskites are vulnerable to moisture, oxygen, UV light, heat, and other potentially external factors.⁶ The encapsulating technology and UV filter can effectively block the ambient environment and protect perovskite crystals from rapid decomposition.⁷ The intrinsic instability of perovskite materials under heat stress is still an evitable issue in practical implementations.

To date, researchers have primarily focused on the stability of PSCs under room temperature or a fixed temperature such as 85 °C for an accelerated aging process to rapidly screen PSC stability,⁸ and extrapolate the potential lifetime.⁹ In various practical application scenarios, temperature fluctuations occur with day and night cycles, seasonal changes, latitude differences, and terrain influences.^{10,11} These

fluctuations can easily induce phase transitions and lattice strain in halide perovskite materials,^{12,13} ultimately leading to irreversible degradation in device performance. The degradation at different temperatures may not be fully observable when assessed along a fixed temperature pathway.¹⁴ Therefore, summarizing and comprehending the working and failure mechanisms of perovskites and their devices during thermal cycling is crucial for developing robust device structures and improving their photovoltaic stability. This understanding is particularly significant for advancing the commercialization of PSCs.

In this perspective, we examined the effects of temperature cycling on the structure and crystal phase of perovskite, as well as the relationship between the charge transport capability and thermal stability of the charge transport layers (CTLs) and the overall temperature stability of PSCs. This allowed us to systematically analyze the impact of temperature cycling on various device parameters.

Building on these attenuation mechanisms, we outlined several strategies for enhancing the temperature stability of the device, focusing on the perovskite light absorption layer, CTLs, and electrodes. Finally, we share some future challenges related to the commercialization of temperature-resistant PSCs.

II. THE EFFECT OF TEMPERATURES ON THE DEGRADATION MECHANISM OF PSCS

Temperature is an important parameter to evaluate the stability of perovskite photovoltaic devices because the temperature during devices' actual operation can easily exceed the room temperature.¹⁵ Traditionally, the thermal stability of PSCs is usually associated with a fixed high temperature since elevated temperatures can hasten the degradation of perovskites and devices. Specifically, perovskites that contain methylammonium cations (MA^+) and iodine (I^-) undergo degradation through processes such as gaseous decomposition, phase transitions, and the formation of ionic defects.¹⁶ Normally, the commonly used organic hole selective layers in p-i-n PSCs such as ultrathin self-assembled monolayers displayed inadequate thermal stability, as the bond between the anchoring group and the molecule's spacer can be disrupted by desorption induced by temperature changes.¹⁷ The damage mechanism of perovskite films and device performance caused by high temperatures has been extensively studied, while the attenuation under variable temperature conditions has rarely been studied. Investigating the impact of temperature fluctuations on the evolution of perovskite structure and device transport layers and interfaces is a top priority for the commercial application of PSCs.

A. Perovskite structure and phase evolution

Since perovskite is a soft lattice material, it will produce greater response to perturbations from temperature change.^{18,19} The heat-induced degradation of perovskite materials can be understood through the Goldschmidt tolerance factor (t), which is an empirical indicator of perovskite crystal stability based on the ionic radius within the crystal. Perovskite materials demonstrate good stability with a tolerance factor ranging from 0.8 to 1.0. However, significant heat-induced degradation occurs when the t value falls outside this range, leading to lattice distortion.²⁰ Temperature variations will cause perovskite octahedral distortions that lead to alterations in its vibrational properties.²¹ Specifically, the variations in vibrations of all atomic sites between the high-temperature and low-temperature phases result in substantial entropy changes, which serve as the primary driving force for phase transition.²² These alterations in the perovskite structure and phase transitions that occur with temperature fluctuations are also closely linked to the specific perovskite components and systems.^{23–25} For example, the classical MAPbI_3 (MA =methylammonium) perovskite crystallizes in a tetragonal phase at room temperature. Additionally, this hybrid perovskite experiences two phase transitions at 160 K (-113.15°C) and 330 K (56.85°C), resulting in crystal structures with higher symmetry. The low-temperature transition is characterized by a shift from an orthorhombic structure (Pna_2_1 space group) to a tetragonal structure ($\text{I}4/\text{mcm}$ space group). In contrast, the high-temperature transition involves a transformation from the tetragonal phase to a cubic phase with $\text{Pm}\bar{3}\text{m}$ space group symmetry.^{26,27} The solution-deposited FAPbI_3 initially forms a hexagonal precursor phase ($\text{P}6_3\text{mc}$ space group), which transforms into the perovskite trigonal phase ($\text{P}3\text{m}1$ space group) upon annealing at temperatures above 130 °C. When annealed for an extended period or at sufficiently high temperatures, the sample degrades into PbI_2 , transitioning to the $\text{P}\bar{3}\text{m}1$ phase.²⁸ The all-inorganic CsPbI_3 perovskite crystallizes in a yellow orthorhombic phase at room temperature. As the temperature increases above 448 K (174.85°C), it transforms to a black orthorhombic phase. When the temperature reaches 583 K (309.85°C), it further

undergoes a transformation to a cubic perovskite phase with $\text{Pm}\bar{3}\text{m}$ space group symmetry.^{27,29,30} The mixed-cation FAMACs-based perovskite (FA =formamidinium) crystallizes in a cubic phase at room temperature. As the temperature decreases to 220 K (-53.15°C), a tetragonal phase emerges.³¹ For temperature up to 423 K (149.85°C), the cubic phase remains highly stable, and no orthorhombic phase transition occurs.³² The tri-cation CsFAMA -based perovskite demonstrates better temperature tolerance for conversion to the orthorhombic phase compared to the purely MA cation-based perovskite. Figure 1(a) provides an overview of the various versatile perovskite structures. The varying composition of the perovskite may contribute to the difference in phase transition, on the one hand, the size and charge of cations and anions affect the stability of their crystal structures. Different cations (such as MA , FA , Cs) have different ionic radii and charges, with different tolerance factors, affecting perovskites' lattice distortion and symmetry.²⁶ On the other hand, composition manipulation can effectively adjust the activation energy of I-Pb bond cleavage and the Pb-I-Pb bond angle in perovskite during the temperature change process, and the $[\text{PbI}_3]^-$ frame deformation energy is also different.^{23,33}

To evaluate the phase transformation process of perovskite during the thermal cycle, *in situ* grazing-incidence wide-angle x-ray scattering (GIWAXS) was implemented. CsFAMA -based perovskites retained the tetragonal phase in the lower temperature range. The degradation products of perovskite during thermal cycling include irreversible PbI_2 , 4H , and 6H phases, along with a reversible tetragonal phase transition, all of which contribute to the deterioration of device performance [Fig. 1(b)].³⁴ Additionally, temperature-dependent x-ray powder diffraction (XRD) measurements were adapted to reveal the crystallographic structure evolution during temperature change processes. As shown in Fig. 1(c), the shift in characteristic peaks of perovskite, the broadening of half-peak width, and the emergence of new characteristic peaks indicate that as the temperature decreases, the perovskite undergoes phase transition and is accompanied by continued distortion of the crystal lattice.³¹ Temperature-dependent Raman spectra were employed to characterize the phase transition process. Temperature fluctuations will weaken H...X interactions and change the orientational states of MA^+ in the PbX_3 cage, causing changes in the bandwidths and peak positions of MA -cage vibrations [Fig. 1(d)].³⁵ These tests provide theoretical support for evaluating the evolution of perovskite structure under variable temperature conditions.

B. Charge transport layers and interface

Temperature cycling generally leads to increased charge carrier recombination, which in turn degrades device performance. It has been reported that inadequate thermostability of CTLs can lead to morphological degradation of perovskite, which subsequently accelerates device deterioration.³⁷ Therefore, the development of efficient and thermo-stable CTLs is crucial for enhancing the thermal stability of these devices.³⁸ Additionally, the mismatch in thermal expansion coefficients (CTEs) between the perovskite and the CTLs results in residual stress within the perovskite as the temperature fluctuates. This leads to significant lattice strain evolution in the perovskite during temperature cycling [Figs. 2(a) and 2(b)].³² Due to the compositional inhomogeneity of the perovskite, these residual stresses are predominantly concentrated at the top of the perovskite and exhibit a gradient distribution in the out-of-plane direction.³⁹ Thermal stress can cause perovskite ion

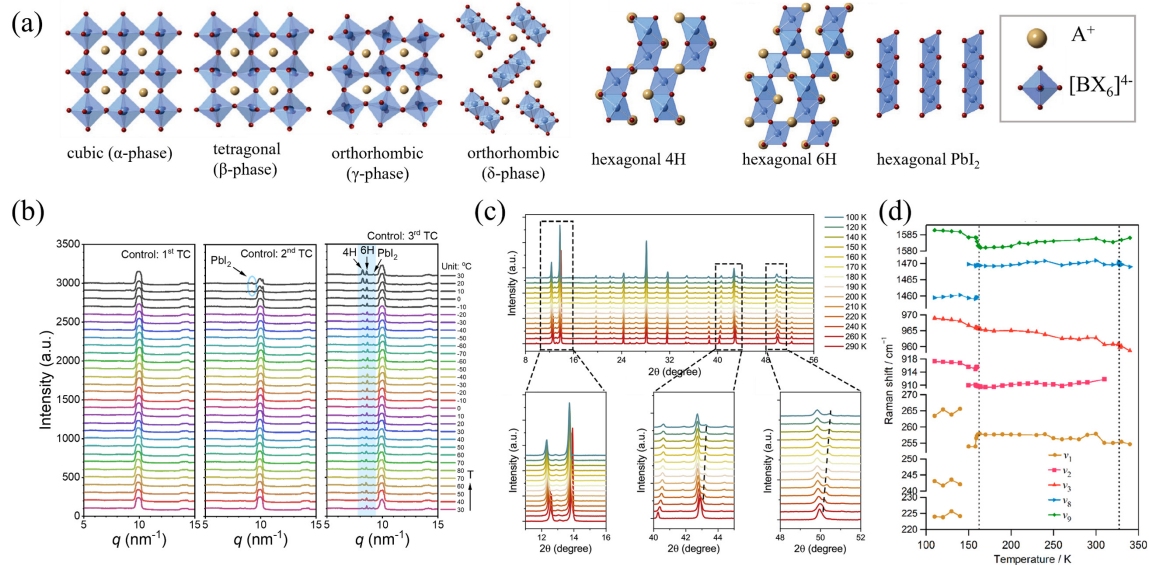


FIG. 1. (a) The various versatile perovskite structures. Reprinted with permission from Lu *et al.*, *Adv. Mater.* **33**, 2105290 (2021). Copyright 2021 Wiley-VCH GmbH.³⁶ (b) The temperature-resolved GIWAXS profiles of FAMACs-based perovskite during thermal cycle processes. Reprinted with permission from Li *et al.*, *Science* **379**, 399–403 (2023). Copyright 2023 American Association for the Advancement of Science.³⁴ (c) XRD patterns as a function of the temperature of FAMACs-based perovskite films. Reprinted with permission from Zhou *et al.*, *Joule* **4**, 1961–1976 (2020). Copyright 2020 Elsevier Inc.³¹ (d) Temperature dependence of peak positions of the Raman bands of MAPbI₃. Reprinted with permission from Furukawa *et al.*, *Molecules* **24**, 626 (2019). Copyright 2020 the Creative Commons Attribution (CCBY) license.³⁵

migration and damage device performance.⁴⁰ Besides that, temperature cycling can induce the migration of perovskite ions to the electrode [Fig. 2(c)], resulting in reactions between the perovskite and the metal electrode, which ultimately leads to device degradation, forming AgI and reducing Pb²⁺ to Pb⁰.⁴¹ Therefore, inhibiting the migration of perovskite ions is crucial for enhancing the temperature stability of perovskite materials.

III. THE EFFECTS OF VARIABLE TEMPERATURE CONDITIONS ON DEVICE PERFORMANCE

Preliminary studies indicate that the device operates optimally at room temperature, with performance degrading when temperatures are either increased or decreased.^{42,43} The device's performance is typically assessed using parameters such as open circuit voltage (V_{OC}), short circuit current density (J_{SC}), fill factor (FF), power conversion efficiency (PCE), and hysteresis index (HI).

We evaluate the impact of temperature fluctuations on device performance through changes in these parameters. As the temperature decreases from room temperature to -160°C , V_{OC} increases, while J_{SC} remains relatively stable. However, FF shows a continuous decline, leading to a reduction in device efficiency. On the other hand, when the temperature rises to 150°C , V_{OC} decreases, contributing to a further reduction in PCE. Despite this, the increase in FF helps mitigate the efficiency loss, and J_{SC} exhibits only minor fluctuations. This indicates that V_{OC} and FF are the primary factors influencing device performance under varying temperature conditions [Fig. 3(a)]. The increase in V_{OC} at low temperatures is attributed to the reduction of defects in both the perovskite bulk phase and at the interface, which improves the device's voltage output.⁴⁴ Conversely, the decline in FF at low temperatures is primarily due to the reduced charge extraction

capability of the CTLs, which increases the series resistance (Rs).^{31,44} When the temperature increases to 150°C , the decrease in V_{OC} is primarily due to an increase in thermally excited carrier density, causing the increase in reverse saturation current and recombination.⁴⁵ Moreover, by comparing the PCE of the forward and reverse sweeps of the device under varying temperature conditions, it can be demonstrated that hysteresis is negatively correlated with temperature [Fig. 3(b)]. In low-temperature environments, the charge transfer capacity of CTLs is reduced, leading to increased hysteresis, which negatively impacts both the efficiency and stability of devices. At high temperatures, perovskite materials may undergo phase transition and decomposition of components (such as methylamine ions), resulting in a device degradation rate of about $0.12\%/\text{°C}$.⁴⁶ During temperature cycling, perovskite lattices may repeatedly experience thermal expansion and contraction, which can lead to stress accumulation and structural damage, thus affecting their stability. Combined with mismatch in the coefficient of thermal expansion between different layers, it can cause interfacial sliding, delamination of layers, and formation of voids. These effects ultimately lead to mechanical failure and material degradation in PSCs.⁴⁷ While this decay is reversible after a limited number of cycles [Fig. 3(c)], the performance degradation resulting from chemical decomposition in the perovskite after multiple cycles is irreversible.^{32,48}

IV. STRATEGIES

The stability of perovskite photovoltaic devices under temperature cycling is mainly related to various factors such as the inherent stability of the perovskite material, the CTL interface, and the material/electrode interface. Several strategies have been developed to stabilize the perovskite phase, including modulating the perovskite

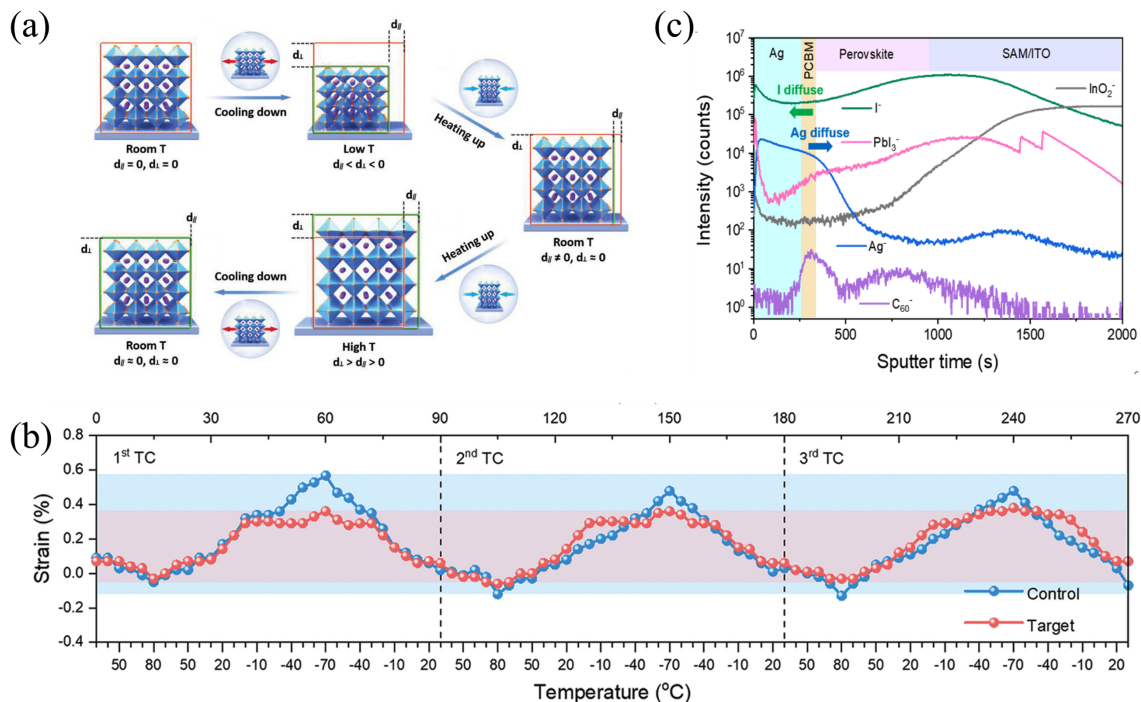


FIG. 2. (a) Schematic of the evolution of the perovskite film strain with temperature. Reprinted with permission from Li *et al.*, *Adv. Energy Mater.* **12**, 2202887 (2022). Copyright 2021 Wiley-VCH GmbH.³² (b) The temperature-resolved lattice strain for perovskites. Reprinted with permission from Li *et al.*, *Science* **379**, 399–403 (2023). Copyright 2023 American Association for the Advancement of Science.³⁴ (c) ToF-SIMS ion species depth profiles of Ag⁻ (Ag), C₆₀⁻ (PCBM), I⁻, Pbl₃⁻ (perovskite), CF₂⁻ (β -pV2F), and InO₂⁻ (ITO) of devices after thermal cycles. Reprinted with permission from Li *et al.*, *Science* **379**, 399–403 (2023). Copyright 2023 American Association for the Advancement of Science.³⁴

composition, using photochemically and thermally stable organic materials as capping layers, employing highly conductive and thermally stable CTls, and other approaches.

As the core light-absorbing layer of the device, the perovskite layer significantly contributes to thermal attenuation of the device due to its inherent instability.⁴⁹ Component engineering can affect the energy bands, crystal phases, efficiency, and stability of perovskite materials, making it an effective strategy for enhancing the temperature stability of PSCs.⁵⁰ To enhance the operational stability of PSCs at higher temperatures, FA and Cs have been utilized to replace MA. This substitution is attributed to their greater enthalpy and activation energy for decomposition reactions.⁵¹ The introduction of Rb into perovskite can effectively inhibit the formation of RbPbI₃ from PbI₂ caused by thermal stress, thereby improving the device's thermal stability.⁵² Additionally, the crystallization and growth processes of solution-processed perovskite films are complex, resulting in diverse crystal orientations and morphologies that can significantly impact device performance. During temperature fluctuations, thermal stress can also induce strain in the perovskite lattice, adversely affecting device performance. Consequently, stabilizing the perovskite lattice is crucial for enhancing the device's thermal stability. A polymer dipole β -poly(1,1-difluoroethylene) (β -pV2F) with a highly ordered dipolar structure can interact with certain perovskite components, promoting the formation of a low-defect crystalline film by lowering the formation energy of the black photoactive phase and facilitating optimal

energy alignment with the charge-selective contacts in the device. The formation of dipoles at the perovskite surface suppresses ion migration, promotes interfacial charge extraction, acts as a buffer for thermal strain, and significantly improves the device's temperature cycling stability (Fig. 4).³⁴

Temperature easily triggers the reaction between the commonly used rear Ag electrode and the halide anion in the perovskite, which will break the thermodynamic balance that affects the reaction of perovskite components, resulting in device performance degradation.⁵³ Replacing the Ag electrode with other chemically inert electrodes in relation to halide perovskites can inhibit the migration of halide ions and Ag diffusion.⁵³ Cu was employed in the p-i-n device without an ETL. It is noteworthy that, despite being annealed for an extended period at 80 °C, Cu did not form CuI and did not contaminate the perovskite layer.⁵⁴

Temperature fluctuations can also lead to decomposition of the CTls and the accumulation of interfacial charges, which accelerates the degradation of device performance.⁵⁵ Therefore, enhancing the stability of charge transfer materials, facilitating charge transfer, and inhibiting interfacial charge accumulation are effective strategies for improving the stability of devices under variable temperature conditions. For instance, C₆₀ is widely employed as an ETL in inverted PSCs due to its excellent electron mobility and its capacity to passivate anti-site defects on the perovskite surface. However, during repeated thermal evaporation processes, the presence of oxygen in the initial

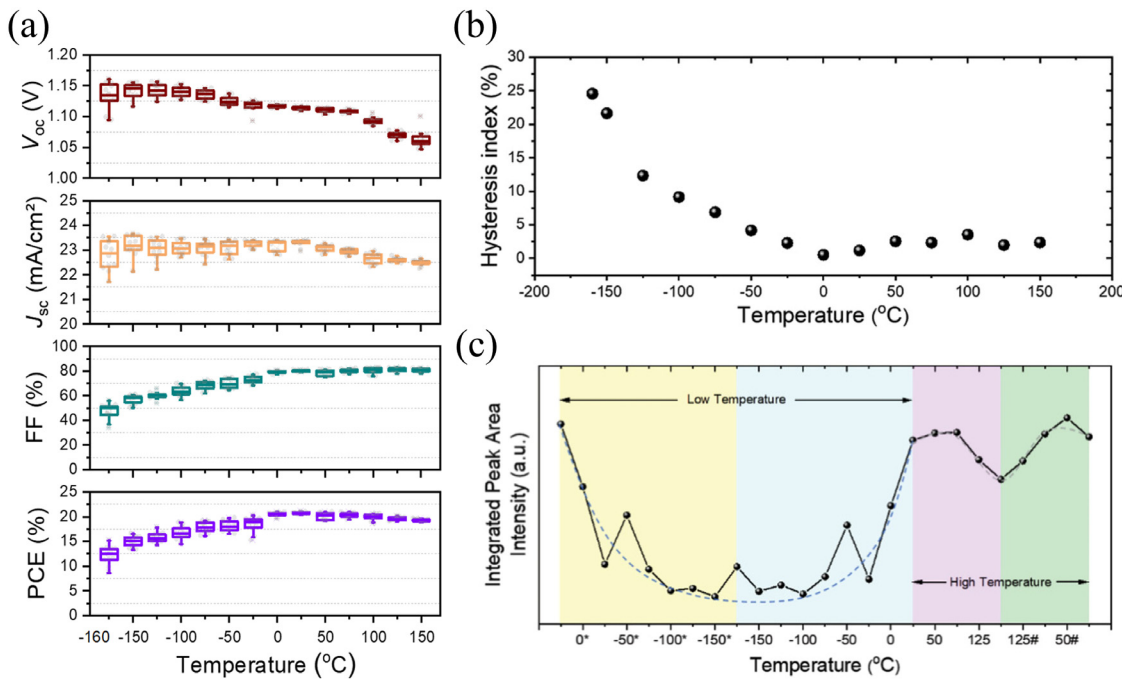


FIG. 3. (a) Statistical box charts of V_{oc} , J_{sc} , FF, and PCE distribution of PSCs at various temperatures. Reprinted with permission from Li *et al.*, *Adv. Energy Mater.* **12**, 2202887 (2022). Copyright 2021 Wiley-VCH GmbH.³² (b) Hysteresis index of PSCs under various temperatures. Reprinted with permission from Li *et al.*, *Adv. Energy Mater.* **12**, 2202887 (2022). Copyright 2021 Wiley-VCH GmbH.³² (c) Temperature-dependent area under the (001) diffraction peak of perovskite films based on GIWAXS measurement. Reprinted with permission from Li *et al.*, *Adv. Energy Mater.* **12**, 2202887 (2022). Copyright 2021 Wiley-VCH GmbH.³²

04 January 2025 05:54:50

material can lead to the formation of deep defect states in perovskites. Additionally, C_{60} can easily convert into higher molecular structures, adversely affecting its electronic properties and compromising device performance. To address these issues, purifying the C_{60} material using a vacuum thermal gradient sublimation method, along with enhancing the molecular thermal stability of C_{60} , can significantly improve device efficiency and stability.⁵⁶ Nickel oxide (NiO_x), known for its exceptional stability and high optical transparency, stands out as the most promising candidate for the hole transport material (HTM) in highly efficient and stable p-i-n PSCs. The significant energy band offset and the high defect density present at the NiO_x /perovskite interface cause significant charge recombination and thermal instability in inverted PSCs. Therefore, incorporating alkali halides, organic monomolecules with high electron affinity, and polar molecules as interfacial passivation layers presents a promising strategy to improve device efficiency by modifying the work function of NiO_x and passivating interfacial defects.^{57–59} Additionally, the intermediate layer can physically separate the NiO_x and perovskite layers, thereby directly inhibiting redox reactions. Ni^{2+} metal cation sites in NiO_x thin films function as both Brønsted proton acceptors and Lewis electron acceptors. They facilitate the deprotonation of cationic amines and oxidize iodide species, leading to the formation of $PbI_{2-x}Br_x$ hole extraction barriers at the interface, this reaction is particularly enhanced at elevated temperatures. Adding 1–5 mol. % excess A-site cation to the perovskite precursor solution can titrate the surface oxide proton-acceptor sites, effectively removing the hole extraction barrier. This adjustment is sufficient to compensate for the loss of the organic cation, preventing the formation

of a $PbI_{2-x}Br_x$ layer at the interface and resulting in a V_{oc} increase of over 200 mV.⁶⁰ Research shows that chiral-structured perovskite interlayers, featuring dynamically stable chiral packing, significantly improve the mechanical, chemical, and charge extraction properties of the ETL/perovskite heterointerface, improving the thermal cycling stability of devices.⁴⁷

V. CONCLUSIONS AND OUTLOOK

Temperature stability poses a significant challenge to the commercial development of PSCs. In this perspective, we discussed the phase transition of perovskite under variable temperature. During the thermal cycling process, the degradation products of perovskite include irreversible PbI_2 , as well as 4H and 6H phases. Additionally, a reversible phase transition occurs, all of which contribute to the decline in device performance. Simultaneously, under conditions of temperature fluctuation, the mismatch in thermal expansion coefficients between the perovskite layer and the CTL leads to residual stress in the perovskite. This stress prompts the migration of perovskite ions, resulting in reactions between the perovskite, the CTL, and the metal electrodes, ultimately degrading device performance. Additionally, charge accumulation is likely to occur at the interfaces of perovskite solar cells. A CTL with high charge transport capacity and thermal stability can effectively mitigate the accumulation of interface charges, enhancing the device's resilience to temperature fluctuations. Subsequently, we discuss the strategies to enhance device temperature stability through approaches such as component engineering and interface

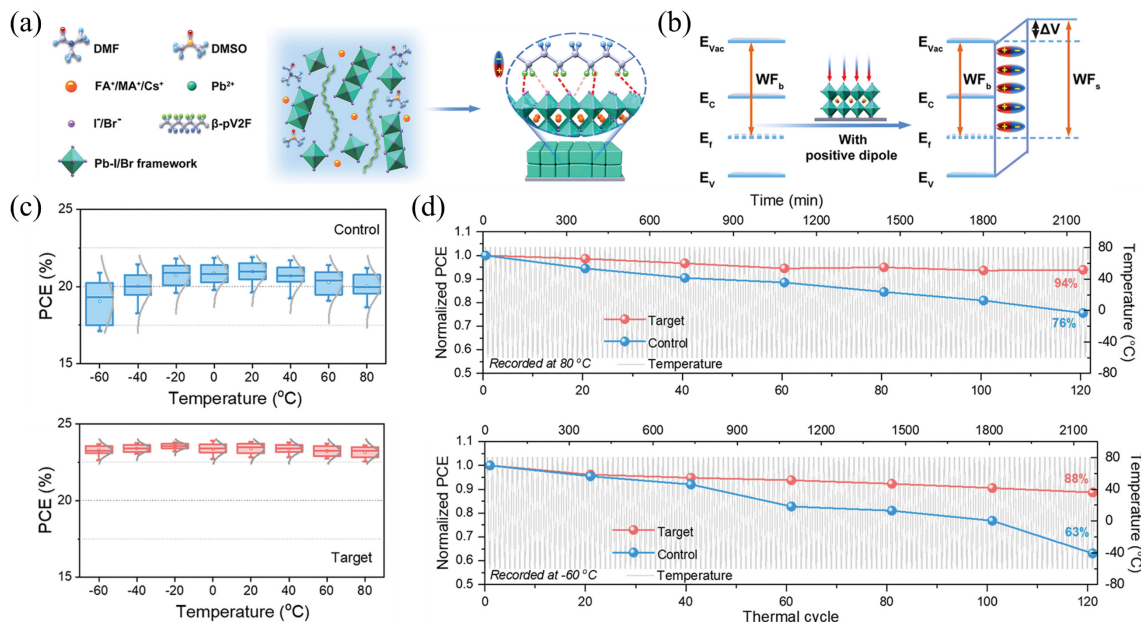


FIG. 4. (a) Schematic of the working mechanism between β -PV2F and perovskite. Reprinted with permission from Li *et al.*, Science **379**, 399–403 (2023). Copyright 2023 American Association for the Advancement of Science.³⁴ (b) Regulation of perovskite work function by β -PV2F. Reprinted with permission from Li *et al.*, Science **379**, 399–403 (2023). Copyright 2023 American Association for the Advancement of Science.³⁴ (c) Statistical temperature dependence PCE profiles of PSCs. Reprinted with permission from Li *et al.*, Science **379**, 399–403 (2023). Copyright 2023 American Association for the Advancement of Science.³⁴ (d) PCE evolution recorded at +80 and -60 °C of PSCs against thermal cycle between -60 and +80 °C. Reprinted with permission from Li *et al.*, Science **379**, 399–403 (2023). Copyright 2023 American Association for the Advancement of Science.³⁴

04 January 2025 0:54:50

optimization. Based on the mechanism of device temperature change and attenuation, we summarized some strategies to improve the thermal cycle stability of PSCs.

First, we can improve the perovskite composition by using components with a larger decomposition reaction enthalpy, such as FA and Cs, in place of MA. Additionally, introducing highly ordered dipole materials can help regulate perovskite crystallization, stabilize the perovskite lattice, and lower the formation energy of the perovskite photoactive phase.

Second, utilizing a charge transport layer with high conductivity and excellent thermal stability can effectively suppress interface charge accumulation and minimize the thermal decomposition of the CTL. Additionally, employing substrates with CTE values that closely match those of the perovskite and incorporating a buffer layer can help to alleviate any CTE or lattice mismatches between the perovskite and the substrate.

Third, replacing the Ag electrode with other chemically inert electrodes can help inhibit the migration of halide ions and the diffusion of Ag in halide perovskites.

Initial studies in this field have established a promising foundation for characterizing and addressing these thermal decompositions; however, significant areas remain unexplored. For instance, devices are subjected to thermal fluctuations, which lead to stress variations due to differing CTEs between the perovskite and substrate. How do PSCs manage these stress fluctuations over time? In other words, a comprehensive understanding of the self-healing mechanisms of devices at low temperatures or room temperature during thermal cycling is essential.

Simultaneously, to more effectively investigate the actual operating conditions of the device, it is important to consider factors such as ultraviolet light exposure and humidity fluctuations, in addition to temperature cycling. This perspective aims to offer a concise overview of temperature-stable PSCs, with the hope of sparking interest and inspiring new ideas in this emerging area of research.

ACKNOWLEDGMENTS

The authors acknowledged the financial support from Zhongyuan Scholar of Henan Province (No.224000510007). This work was supported by the Joint Fund of Provincial Science and Technology Research, Development Plan of Henan Province (No. 232301420004), and the Outstanding Youth Fund of the Natural Science Foundation of Henan Province (No.242300421069).

AUTHOR DECLARATIONS

Conflict of Interest

The authors have no conflicts to disclose.

Author Contributions

Ying Tang: Investigation (lead); Methodology (lead); Writing – original draft (lead). **Yufang Liu:** Conceptualization (lead); Funding acquisition (lead); Investigation (equal); Supervision (lead). **Meng Li:** Conceptualization (supporting); Funding acquisition (lead); Supervision (equal); Writing – review & editing (supporting).

DATA AVAILABILITY

The data that support the findings of this study are available from the corresponding authors upon reasonable request.

REFERENCES

- ¹H. Zhu, S. Teale, M. N. Lintangpradipo, S. Mahesh, B. Chen, M. D. McGehee, E. H. Sargent, and O. M. Bakr, *Nat. Rev. Mater.* **8**, 569 (2023).
- ²A. S. R. Bati, Y. L. Zhong, P. L. Burn, M. K. Nazeruddin, P. E. Shaw, and M. Batmunkh, *Commun. Mater.* **4**, 2 (2023).
- ³National Renewable Energy Laboratory, see <https://www.nrel.gov/pv/assets/pdfs/best-research-cell-efficiencies.pdf> 2024 for “Best Research-Cell Efficiency Chart”; accessed: 2024-10-24.
- ⁴H. Gu, J. Xia, C. Liang, Y. Chen, W. Huang, and G. Xing, *Nat. Rev. Mater.* **8**, 533 (2023).
- ⁵J. You, L. Meng, T.-B. Song, T.-F. Guo, Y. Yang, W.-H. Chang, Z. Hong, H. Chen, H. Zhou, Q. Chen, Y. Liu, N. De Marco, and Y. Yang, *Nat. Nanotechnol.* **11**, 75 (2016).
- ⁶T. Leijtens, G. E. Eperon, N. K. Noel, S. N. Habisreutinger, A. Petrozza, and H. J. Snaith, *Adv. Energy Mater.* **5**, 1500963 (2015).
- ⁷N. Ahn, K. Kwak, M. S. Jang, H. Yoon, B. Y. Lee, J.-K. Lee, P. V. Pikhitsa, J. Byun, and M. Choi, *Nat. Commun.* **7**, 13422 (2016).
- ⁸X. Zhao, T. Liu, Q. C. Burlingame, T. Liu, R. Holley, G. Cheng, N. Yao, F. Gao, and Y.-L. Loo, *Science* **377**, 307 (2022).
- ⁹K. Zhao, Q. Liu, L. Yao, C. Değer, J. Shen, X. Zhang, P. Shi, Y. Tian, Y. Luo, J. Xu, J. Zhou, D. Jin, S. Wang, W. Fan, S. Zhang, S. Chu, X. Wang, L. Tian, R. Liu, L. Zhang, I. Yavuz, H.-F. Wang, D. Yang, R. Wang, and J. Xue, *Nature* **632**, 301 (2024).
- ¹⁰A. Munguira, R. Hueso, A. Sánchez-Lavega, M. de la Torre-Juarez, G. M. Martínez, C. E. Newman, E. Sebastian, A. Lepinette, A. Vicente-Retortillo, B. Chide, M. T. Lemmon, T. Bertrand, R. D. Lorenz, D. Banfield, J. Gómez-Elvira, J. Martín-Soler, S. Navarro, J. Pla-García, J. A. Rodríguez-Manfredi, J. Romeral, M. D. Smith, and J. Torres, *J. Geophys. Res.: Planets* **128**, e2022JE007559, <https://doi.org/10.1029/2022JE007559> (2023).
- ¹¹Z. Wang, Y. Li, K. Wang, and Z. Huang, *Renewable Sustainable Energy Rev.* **76**, 1153 (2017).
- ¹²Y. Jiao, S. Yi, H. Wang, B. Li, W. Hao, L. Pan, Y. Shi, X. Li, P. Liu, H. Zhang, C. Gao, J. Zhao, and J. Lu, *Adv. Funct. Mater.* **31**, 2006243 (2021).
- ¹³M.-J. Choi, J.-W. Lee, and H. W. Jang, *Adv. Mater.* **36**, 2308827 (2024).
- ¹⁴M. Jošt, B. Lipovšek, B. Glažar, A. Al-Ashouri, K. Brelc, G. Matič, A. Magomedov, V. Getautis, M. Topič, and S. Albrecht, *Adv. Energy Mater.* **10**, 2000454 (2020).
- ¹⁵I. Mesquita, L. Andrade, and A. Mendes, *ChemSusChem* **12**, 2186 (2019).
- ¹⁶D. Lan and M. A. Green, *Joule* **6**, 1782 (2022).
- ¹⁷Z. Li, X. Sun, X. Zheng, B. Li, D. Gao, S. Zhang, X. Wu, S. Li, J. Gong, J. M. Luther, Z. A. Li, and Z. Zhu, *Science* **382**, 284 (2023).
- ¹⁸J. M. Frost, K. T. Butler, and A. Walsh, *APL Mater.* **2**, 081506 (2014).
- ¹⁹B. Conings, J. Drijkoningen, N. Gauquelin, A. Babayigit, J. D'Haen, L. D'Olielaeger, A. Ethirajan, J. Verbeeck, J. Manca, E. Mosconi, F. D. Angelis, and H.-G. Boyen, *Adv. Energy Mater.* **5**, 1500477 (2015).
- ²⁰W. Chi and S. K. Banerjee, *Chem. Mater.* **33**, 1540 (2021).
- ²¹T. Pandey, M.-H. Du, D. S. Parker, and L. Lindsay, *Mater. Today Phys.* **28**, 100881 (2022).
- ²²W. Wei, W. Li, K. T. Butler, G. Feng, C. J. Howard, M. A. Carpenter, P. Lu, A. Walsh, and A. K. Cheetham, *Angew. Chem., Int. Ed.* **57**, 8932 (2018).
- ²³L. Cojocaru, S. Uchida, Y. Sanehira, V. Gonzalez-Pedro, J. Bisquert, J. Nakazaki, T. Kubo, and H. Segawa, *Chem. Lett.* **44**, 1557 (2015).
- ²⁴S. Thakur and A. Giri, *ACS Appl. Mater. Interfaces* **15**, 26755 (2023).
- ²⁵Z.-A. Nan, L. Chen, Q. Liu, S.-H. Wang, Z.-X. Chen, S.-Y. Kang, J.-B. Ji, Y.-Y. Tan, Y. Hui, J.-W. Yan, Z.-X. Xie, W.-Z. Liang, B.-W. Mao, and Z.-Q. Tian, *Chem* **7**, 2513 (2021).
- ²⁶T. T. Ava, A. Al Mamun, S. Marsillac, and G. Namkoong, *Appl. Sci.* **9**, 188 (2019).
- ²⁷A. Bonadio, F. P. Sabino, A. L. M. Freitas, M. R. Felez, G. M. Dalpian, and J. A. Souza, *Inorg. Chem.* **62**, 7533 (2023).
- ²⁸V. L. Pool, B. Dou, D. G. Van Campen, T. R. Klein-Stockert, F. S. Barnes, S. E. Shaheen, M. I. Ahmad, M. F. A. M. van Hest, and M. F. Toney, *Nat. Commun.* **8**, 14075 (2017).
- ²⁹R. J. Sutton, M. R. Filip, A. A. Haghhighirad, N. Sakai, B. Wenger, F. Giustino, and H. J. Snaith, *ACS Energy Lett.* **3**, 1787 (2018).
- ³⁰T. Braeckeveldt, R. Goeminne, S. Vandenhante, S. Borgmans, T. Verstraelen, J. A. Steele, M. B. J. Roeffaers, J. Hofkens, S. M. J. Rogge, and V. Van Speybroeck, *Chem. Mater.* **34**, 8561 (2022).
- ³¹Y. Chen, S. Tan, N. Li, B. Huang, X. Niu, L. Li, M. Sun, Y. Zhang, X. Zhang, C. Zhu, N. Yang, H. Zai, Y. Wu, S. Ma, Y. Bai, Q. Chen, F. Xiao, K. Sun, and H. Zhou, *Joule* **4**, 1961 (2020).
- ³²G. Li, Z. Su, M. Li, H. K. H. Lee, R. Datt, D. Hughes, C. Wang, M. Flatken, H. Köbler, J. J. Jerónimo-Rendon, R. Roy, F. Yang, J. Pascual, Z. Li, W. C. Tsoi, X. Gao, Z. Wang, M. Saliba, and A. Abate, *Adv. Energy Mater.* **12**, 2202887 (2022).
- ³³Y. Zhao, J. Zhang, Z. Xu, S. Sun, S. Langner, N. T. P. Hartono, T. Heumueller, Y. Hou, J. Elia, N. Li, G. J. Matt, X. Du, W. Meng, A. Osset, K. Zhang, T. Stubhan, Y. Feng, J. Hauch, E. H. Sargent, T. Buonassisi, and C. J. Brabec, *Nat. Commun.* **12**, 2191 (2021).
- ³⁴G. Li, Z. Su, L. Canil, D. Hughes, M. H. Aldamasy, J. Dagar, S. Trofimov, L. Wang, W. Zuo, J. J. Jerónimo-Rendon, M. M. Byranvand, C. Wang, R. Zhu, Z. Zhang, F. Yang, G. Nasti, B. Naydenov, W. C. Tsoi, Z. Li, X. Gao, Z. Wang, Y. Jia, E. Unger, M. Saliba, M. Li, and A. Abate, *Science* **379**, 399 (2023).
- ³⁵K. Nakada, Y. Matsumoto, Y. Shimoi, K. Yamada, and Y. Furukawa, *Molecules* **24**, 626 (2019).
- ³⁶M. Qin, P. F. Chan, and X. Lu, *Adv. Mater.* **33**, 2105290 (2021).
- ³⁷Z. Zhu, D. Zhao, C.-C. Chueh, X. Shi, Z. Li, and A. K. Y. Jen, *Joule* **2**, 168 (2018).
- ³⁸A. D. Sheikh, R. Munir, M. A. Haque, A. Bera, W. Hu, P. Shaikh, A. Amassian, and T. Wu, *ACS Appl. Mater. Interfaces* **9**, 35018 (2017).
- ³⁹H. Zhang and N.-G. Park, *Angew. Chem., Int. Ed.* **61**, e202212268 (2022).
- ⁴⁰T. Tayagaki, S. Hirooka, H. Kobayashi, K. Yamamoto, T. N. Murakami, and M. Yoshita, *Sol. Energy Mater. Sol. Cells* **272**, 112879 (2024).
- ⁴¹X. Li, H.-H. Ding, G.-H. Li, Y. Wang, Z.-M. Fang, S.-F. Yang, H.-X. Ju, and J.-F. Zhu, *Chin. J. Chem. Phys.* **32**, 299 (2019).
- ⁴²J. A. Schwenzer, L. Rakocevic, R. Gehlhaar, T. Abzieher, S. Gharibzadeh, S. Moghadamzadeh, A. Quintilla, B. S. Richards, U. Lemmer, and U. W. Paetzold, *ACS Appl. Mater. Interfaces* **10**, 16390 (2018).
- ⁴³R. Cao, F. Xu, J. Zhu, S. Ge, W. Wang, H. Xu, R. Xu, Y. Wu, Z. Ma, F. Hong, and Z. Jiang, *Adv. Energy Mater.* **6**, 1600814 (2016).
- ⁴⁴J. Barbé, A. Pockett, V. Stoichkov, D. Hughes, H. K. H. Lee, M. Carnie, T. Watson, and W. C. Tsoi, *J. Mater. Chem. C* **8**, 1715 (2020).
- ⁴⁵A. Kumar, U. Bansode, S. Ogale, and A. Rahman, *Nanotechnology* **31**, 365403 (2020).
- ⁴⁶S. M. Park, M. Wei, J. Xu, H. R. Atapattu, F. T. Eickemeyer, K. Darabi, L. Grater, Y. Yang, C. Liu, S. Teale, B. Chen, H. Chen, T. Wang, L. Zeng, A. Maxwell, Z. Wang, K. R. Rao, Z. Cai, S. M. Zakeeruddin, J. T. Pham, C. M. Risko, A. Amassian, M. G. Kanatzidis, K. R. Graham, M. Grätzel, and E. H. Sargent, *Science* **381**, 209 (2023).
- ⁴⁷T. Duan, S. You, M. Chen, W. Yu, Y. Li, P. Guo, J. J. Berry, J. M. Luther, K. Zhu, and Y. Zhou, *Science* **384**, 878 (2024).
- ⁴⁸A. A. Mamun, T. T. Ava, H. R. Byun, H. J. Jeong, M. S. Jeong, L. Nguyen, C. Gausin, and G. Namkoong, *Phys. Chem. Chem. Phys.* **19**, 19487 (2017).
- ⁴⁹S. S. Dipta and A. Uddin, *Energy Technol.* **9**, 2100560 (2021).
- ⁵⁰J. Dutta, M. Chennamkulam Ajith, S. Dutta, U. R. Kadhande, J. Kochupurackal B, and B. Rai, *Sci. Rep.* **10**, 15241 (2020).
- ⁵¹E. J. Juarez-Perez, L. K. Ono, and Y. Qi, *J. Mater. Chem. A* **7**, 16912 (2019).
- ⁵²T. Matsui, T. Yamamoto, T. Nishihara, R. Morisawa, T. Yokoyama, T. Sekiguchi, and T. Negami, *Adv. Mater.* **31**, 1806823 (2019).
- ⁵³J. Zhou, Z. Liu, P. Yu, G. Tong, R. Chen, L. K. Ono, R. Chen, H. Wang, F. Ren, S. Liu, J. Wang, Z. Lan, Y. Qi, and W. Chen, *Nat. Commun.* **14**, 6120 (2023).
- ⁵⁴J. Zhao, X. Zheng, Y. Deng, T. Li, Y. Shao, A. Gruverman, J. Shield, and J. Huang, *Energy Environ. Sci.* **9**, 3650 (2016).
- ⁵⁵M. T. Mbumba, D. M. Malouangou, J. M. Tsiba, L. Bai, Y. Yang, and M. Guli, *Sol. Energy* **230**, 954 (2021).
- ⁵⁶A. A. Said, E. Aydin, E. Ugur, Z. Xu, C. Deger, B. Vishal, A. Vlk, P. Dally, B. K. Yildirim, R. Azmi, J. Liu, E. A. Jackson, H. M. Johnson, M. Gui, H. Richter, A. R. Pininti, H. Bristow, M. Babics, A. Razzaq, T. G. Allen, M. Ledinský, I. Yavuz, B. P. Rand, and S. D. Wolf, *Nat. Commun.* **15**, 708 (2024).
- ⁵⁷W. Chen, Y. Zhou, G. Chen, Y. Wu, B. Tu, F.-Z. Liu, L. Huang, A. M. C. Ng, A. B. Djurišić, and Z. He, *Adv. Energy Mater.* **9**, 1803872 (2019).

⁵⁸L. Li, X. Zhang, H. Zeng, X. Zheng, Y. Zhao, L. Luo, F. Liu, and X. Li, *Chem. Eng. J.* **443**, 136405 (2022).
⁵⁹Y. Wu, M. Wei, Y. Sun, X. Yang, W. Xun, M. Li, R. Chen, Y. Lin, P. Li, and Q.-S. Jiang, *Vacuum* **222**, 113057 (2024).

⁶⁰C. C. Boyd, R. C. Shallcross, T. Moot, R. Kerner, L. Bertoluzzi, A. Onno, S. Kavadiya, C. Chosy, E. J. Wolf, J. Werner, J. A. Raiford, C. de Paula, A. F. Palmstrom, Z. J. Yu, J. J. Berry, S. F. Bent, Z. C. Holman, J. M. Luther, E. L. Ratcliff, N. R. Armstrong, and M. D. McGehee, *Joule* **4**, 1759 (2020).